

1 **MOSim: bulk and single-cell multi-layer regulatory network simulator**

2 Carolina Monzó¹, Maider Aguerralde-Martin², Carlos Martínez-Mira³, Ángeles Arzalluz-

3 Luque^{1,2}, Ana Conesa^{1,A}, Sonia Tarazona^{2,A}

4 1. Genomics of Gene Expression Lab, Institute for Integrative Systems Biology, Spanish

5 National Research Council (CSIC-UV), Paterna, 46980, Spain

6 2. Applied Statistics, Operational Research and Quality Department, Universitat

7 Politècnica de València, València, 46022, Spain

8 3. Biobam Bioinformatics S.L., València, 46024, Spain

9 A. Co-corresponding author: sotacam@eio.upv.es and ana.conesa@csic.es

10 **Keywords**

11 Multi-omic simulator, bulk, single-cell, transcriptomics

12 **Key Points**

13 1. MOSim is capable of generating synthetic datasets for a broad spectrum of omics types,
14 supporting bulk RNA-seq, ChIP-seq, ATAC-seq, miRNA-seq, Methyl-seq, and transcription
15 factor data, as well as single-cell omics, including scRNA-seq, scATAC-seq, and
16 transcription factors.

17 2. MOSim enables the robust simulation of complex, many-to-many regulatory relationships
18 across molecular layers, faithfully capturing intricate regulatory patterns.

19 3. Offering extensive options for customization, MOSim's flexible experimental design and
20 parameterization empowers users to simulate count matrices and multilayer regulatory
21 networks, tailoring simulations to diverse experimental scenarios and omics types.

22 Abstract

23 As multi-omics sequencing technologies advance, the need for simulation tools capable of
24 generating realistic and diverse (bulk and single-cell) multi-omics datasets for method testing
25 and benchmarking becomes increasingly important. We present MOSim, an R package that
26 simulates both bulk (via `mosim` function) and single-cell (via `sc_mosim` function) multi-omics
27 data. The `mosim` function generates bulk transcriptomics data (RNA-seq) and additional
28 regulatory omics layers (ATAC-seq, miRNA-seq, ChIP-seq, Methyl-seq and Transcription
29 Factors), while `sc_mosim` simulates single-cell transcriptomics data (scRNA-seq) with
30 scATAC-seq and Transcription Factors as regulatory layers. The tool supports various
31 experimental designs, including simulation of gene co-expression patterns, biological
32 replicates, and differential expression between conditions.

33 MOSim enables users to generate quantification matrices for each simulated omics data type,
34 capturing the heterogeneity and complexity of bulk and single-cell multi-omics datasets.
35 Furthermore, MOSim provides differentially abundant features within each omics layer and
36 elucidates the active regulatory relationships between regulatory omics and gene expression
37 data at both bulk and single-cell levels.

38 By leveraging MOSim, researchers will be able to generate realistic and customizable bulk and
39 single-cell multi-omics datasets to benchmark and validate analytical methods specifically
40 designed for the integrative analysis of diverse regulatory omics data.

41 Introduction

42 Rapid advancements in massive sequencing technologies have significantly facilitated the
43 widespread adoption of multi-omic assays, enabling a comprehensive exploration of the

44 regulatory mechanisms governing biological systems. Consequently, numerous bioinformatics
45 tools have emerged to assist researchers in processing multi-omics data, with a specific focus
46 on unravelling multi-layer gene regulatory networks (GRNs) [1,2]. These GRNs serve as
47 interpretable computational models, providing insights into the intricate regulation of gene
48 expression through interconnected networks. Notably, GRNs encompass diverse regulatory
49 components, including transcription factors (TF), chromatin accessibility, long non-coding
50 RNAs, micro-RNAs, and methylation, among others [2]. Despite the experimental capacity to
51 generate both bulk and single-cell multi-omic sequencing datasets, a significant challenge in
52 GRN studies lies in precisely integrating these multiple omic layers. Therefore, the importance
53 of benchmarking, tuning, and validating multi-omics integration pipelines becomes evident.

54 Synthetic data, serving as ground truth, provides an indispensable resource for defining true
55 positive and negative features sets, enabling rigorous benchmarking, tuning, and validation of
56 analytical methods. Despite the paramount role of synthetic data, there are few publicly
57 available algorithms capable of simulating multiple omic data types. To our knowledge, only
58 three methods support comprehensive multi-omics simulation of gene expression regulation
59 for bulk datasets. The first, the InterSIM R package [3], generates datasets for DNA
60 methylation, gene expression, protein abundance, and their relationships. Although the method
61 allows for customization of the number of biological replicates and the proportion of
62 differentially expressed features, it lacks options for time series simulation and fails to report
63 the interaction among features. The second tool, OmicsSIMLA C++ [4], can simulate
64 genomics, transcriptomics, methylation, and proteomics data. Nevertheless, it restricts the
65 generation of count data matrices to the transcriptomics module and does not include
66 customizable options for time points or replicates. The third tool, the sismonr R package [5],
67 simulates RNA-seq count data in conjunction with pre- and post-transcriptional regulatory
68 networks, offering time-series simulation capabilities. Nonetheless, this method lacks the

69 flexibility to customise expression profiles and dynamics, and the only omic quantification data
70 it generates is gene expression.

71 Given the cell-type-specific nature of regulatory regions, it is surprising that only two methods
72 currently support multi-omics simulation for single-cell datasets. The statistical simulator
73 scDesign3 [6] encompasses scRNA-seq, scATAC-seq, CITE-seq and methylation. Meanwhile,
74 scMultiSim [7] can simulate scRNA-seq and scATAC-seq datasets. While both methods
75 accurately simulate datasets closely resembling real data, none of them provide essential
76 customization options, such as the number of experimental groups, biological replicates,
77 differentially expressed genes, accessible chromatin, and reporting of interaction between
78 features. Importantly, none of these tools is designed to simulate gene regulatory relationships
79 across omics features, which underscores the existing gaps and limitations in current multi-
80 omics simulation tools. GRouNdGAN [8] partially addresses this limitation by modeling GRNs
81 with genes and TFs with single-cell resolution. However, it does not support other omic
82 modalities, multiple experimental conditions, or multiple samples, further underscoring the
83 need for more comprehensive simulation tools.

84 Here we present MOSim, a multi-layer regulatory network simulator for both bulk (RNA-seq,
85 ATAC-seq, miRNA-seq, ChIP-seq and Methyl-seq) and single-cell datasets (scRNA-seq and
86 scATAC-seq), implemented as an R Bioconductor package. In a nutshell, MOSim generates
87 quantification data for each omics layer, precisely controlling active regulatory relationships
88 between regulatory omics and gene expression data for differentially expressed genes.
89 Moreover, MOSim empowers users to customise data generation, enabling the inclusion of
90 experimental groups, biological replicates, time series, and diverse cell types. By harnessing
91 the capabilities of MOSim, bioinformatic tool developers will be able to generate realistic and
92 customizable bulk and single-cell multi-omics datasets, facilitating the benchmarking and

93 validation of analytical methods tailored explicitly for integrating multi-omics data and
94 inference of multi-layer GRNs.

95 **Results**

96 **Overview of MOSim's workflows**

97 MOSim is a bulk and single-cell simulation environment designed for generating multi-omic
98 regulatory networks with precise control over regulator-gene relationships. To create a
99 synthetic ground truth multi-omic dataset, MOSim requires as input the list of omic data types
100 to be simulated, a single sample of seed count data for each of them, and an association file for
101 each regulatory omic type, indicating the *a priori* or potential regulatory features associated
102 with each gene (Figure 1A). While MOSim provides users with example multi-omics datasets
103 to use as seed count data for simulation, the algorithm may also be fed with the user's count
104 dataset of choice, regardless of organism, disease or platform of origin. Besides simulation of
105 RNA-seq or scRNA-seq data depending on the type of study (i.e. bulk or single-cell), currently
106 supported omic regulatory data types include ChIP-seq, miRNA-seq, Methyl-seq, ATAC-seq
107 and scATAC-seq. The algorithm also supports modelling Transcription Factor (TF) - target
108 gene interactions from both bulk and single-cell RNA-seq data.

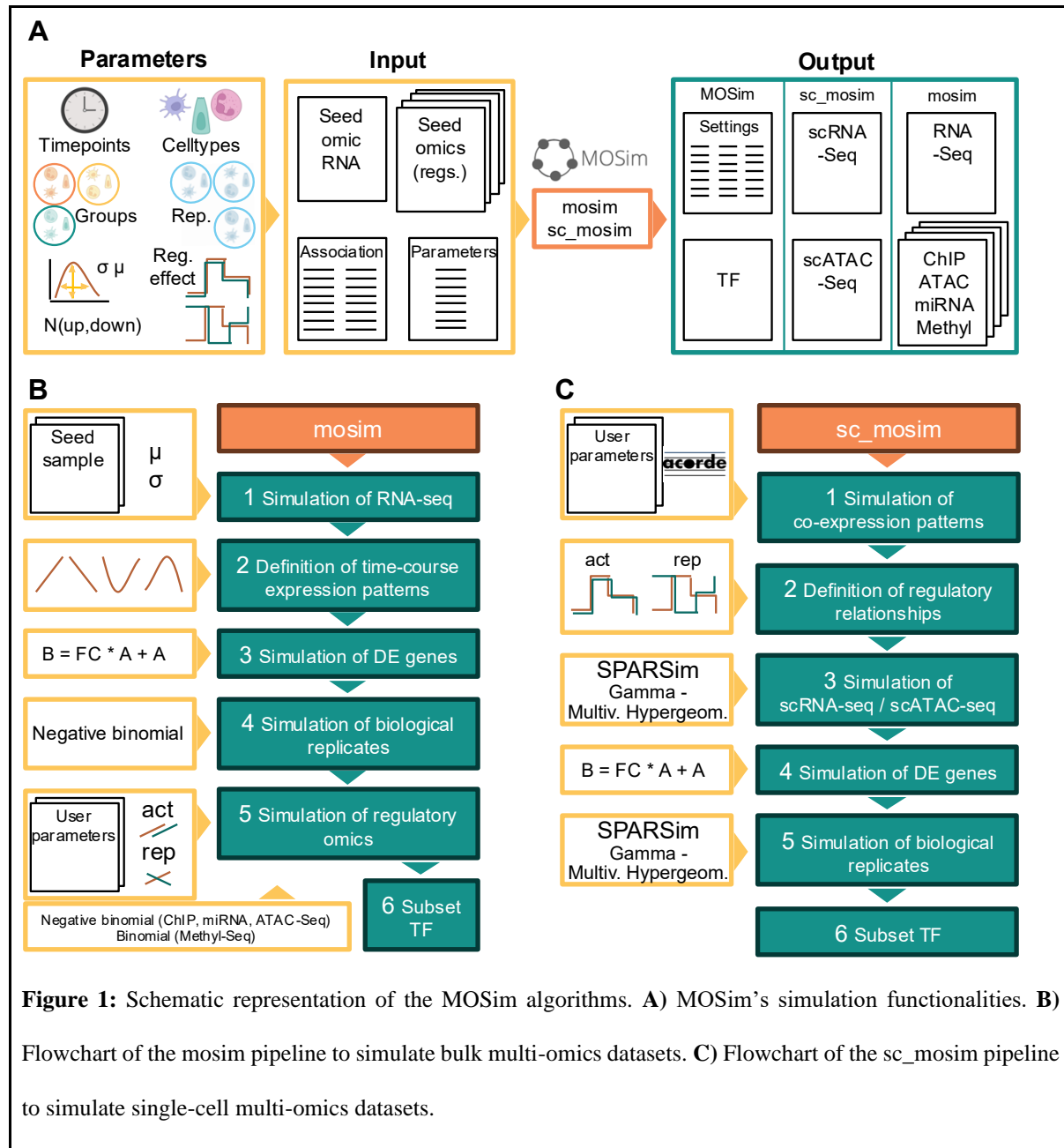
109 Users can define various configuration parameters related to the experimental design, such as
110 the number of experimental groups, time-points or cell types (if applicable), replicates per
111 experimental condition, data dispersion, number of differentially expressed genes and number
112 of regulators with activator or repressor effects. MOSim outputs simulated count matrices for
113 each expression and regulatory data type. Moreover, it generates a record of all parameters
114 used in data creation (MOSim simulated settings), which is indispensable for accurately testing

115 GRN inference bioinformatic tools (i.e. mean expression, dispersion, time profile, fold change
116 etc.) (Figure 1A).

117 The MOSim package includes two main functions: mosim, for bulk datasets simulation, and
118 sc_mosim, for single-cell datasets simulation.

119 The simulation results include three distinct outputs: (i) the simulated omic count data,
120 represented as a matrix for each omic modality. Each matrix contains the same number of omic
121 features as provided in the seed data and the number of samples, groups, cells, etc., specified
122 by the user; (ii) for gene expression, a table listing the genes simulated as differentially
123 expressed, along with their temporal profile (only for bulk; see Table 1); and (iii) a table for
124 each omic modality detailing the regulatory relationships provided by the user, including the
125 simulated activator or repression regulations (see Tables 2 and 3).

126 In addition to the primary MOSim functions for simulating bulk (mosim) or single-cell
127 (sc_mosim) multi-omic datasets, the package provides several other useful functions. These
128 include functions for modifying seed data (omicData and sc_omicData), adjusting default omic
129 parameters (omicSim), and retrieving simulation results and settings (omicResults,
130 omicSettings, sc_omicResults and sc_omicSettings).



131

132 Bulk multi-omic GRNs: the mosim functionality

133 The mosim workflow (Figure 1B) consists of the following steps:

134 1. As the more extended assumption for RNA-seq data, a negative binomial (NB)
135 distribution is applied to generate a bulk RNA-seq count matrix, obtaining the mean

136 and dispersion from the seed sample and the amount of variability across replicates set
137 by the user.

138 2. Differentially expressed genes (DEGs) are randomly selected from the seed RNA-seq
139 sample. DEGs are labelled with one of the following time-course patterns in each
140 experimental group: continuous induction (increasing linear pattern), continuous
141 repression (decreasing linear pattern), transitory induction (quadratic pattern with an
142 intermediate maximum), transitory repression (quadratic pattern with an intermediate
143 minimum), or flat, which is also the default pattern for non-DEGs.

144 3. Expression profiles are simulated based on the seed count values to closely reflect real
145 data distributions. For transitory profiles, the algorithm randomly selects the time point
146 at which the expression reaches its maximum or minimum and simulates a quadratic
147 pattern. For continuous profiles, the algorithm randomly defines both the expression
148 value at the first time point and the slope of change over time, simulating a linear
149 pattern. These patterns vary depending on the coefficient values of the simulation
150 function, particularly as the number of time points increases, and thus, although there
151 are four theoretical temporal profiles, the simulated profiles encompass a wider range
152 of patterns. DEGs with flat profiles or DEGs in a two-group design with no time points
153 are modelled by introducing a fold-change in one of the experimental conditions. For
154 designs with more than two experimental groups, the first serves as the reference and
155 the fold-change is applied to a random selection of the remaining groups.

156 4. After generating gene expression values for each condition, replicates are simulated
157 using a NB distribution.

158 5. All bulk MOSim data types (except Methyl-seq) are assumed to follow a NB
159 distribution. Therefore, the NB is also used to simulate replicates for the remaining
160 omics, but subjected to the simulated settings of the provided regulatory data and a

161 randomly chosen direction of regulation. Regulators labelled as activators adopt the
162 same profile as their associated genes, while repressors follow the opposite pattern.

163 6. For Methyl-seq, proportions are generated instead of counts based on the binomial
164 distribution, following the strategy described in [9]. TF expression values are extracted
165 from the simulated RNA-seq data to simulate TF regulation.

166 A detailed explanation of the bulk mosim algorithm implementation is provided in
167 Supplementary File 1.

168 Single-cell multi-omic GRNs: the sc_mosim functionality

169 The workflow of sc_mosim (Figure 1C) consists of the following steps:

170 1. Following the approach used by the acorde R package for defining isoform profiles
171 across cell types in single-cell RNA-seq [10], gene expression and peak accessibility
172 values in the seed datasets are reorganised to build synthetic features following cross-
173 cell type patterns, i.e., indicating low or high expression in a given cell type.

174 2. Peak accessibility values are rearranged to reflect the regulatory relationship between
175 scRNA-seq and scATAC-seq. Regulators labelled as activators share the same cross-
176 cell type profile as their associated gene, while repressors have the opposite pattern.

177 3. Feature intensity, variability (variance of normalised counts across cells of the same
178 cell type) and library size of the rearranged seed scRNA-seq and scATAC-seq datasets
179 are estimated using SPARSim. A reference dataset is then simulated for each omic data
180 type using a Gamma-Multivariate Hypergeometric model [11].

181 4. DEGs are randomly selected from the reference scRNA-seq. DEGs and their associated
182 differentially accessible peaks between experimental groups are generated by
183 introducing a fold-change in the experimental conditions, using the first condition as

184 the reference. Additionally, random noise is added to the quantification values to
185 introduce realistic variability between experimental groups and across features.

186 5. Feature intensity and library size of the simulated scRNA-seq and scATAC-seq count
187 matrices for each experimental group are estimated using SPARSim. Biological
188 replicates are then simulated using the Gamma-Multivariate Hypergeometric model
189 [11], with the estimated parameters and a small random variability. TF expression
190 values are extracted from the simulated scRNA-seq data to simulate TF regulation.

191 A detailed explanation of the single-cell sc_mosim algorithm implementation is provided in
192 Supplementary File 1.

193 Validation of the bulk (mosim) simulation approach

194 To demonstrate mosim's capabilities for bulk sequencing data, we simulated RNA-seq and
195 ATAC-seq data with five time points, two experimental groups, and three replicates, using the
196 STATegra [12] samples included in the MOSim R package as seed data. We set the number of
197 DEGs to 15% and modelled the five temporal profiles previously described. MOSim returns
198 two types of output. The omicResults function returns a list containing the simulated data
199 matrix for each omic, with features in rows and observations in columns. The second results
200 object, accessible via the omicSettings function, includes the mosim-generated settings for the
201 simulated relationships between gene expression and the rest of omics, as illustrated in Tables
202 1 and 2 containing simulation settings for RNA-seq and ATAC-seq, respectively. For instance,
203 gene ENSMUSG00000052726 is identified as a DEG, displaying transitory repression in
204 condition 1 and transitory induction in condition 2. The chromatin-accessible region
205 1_140257767_140257897 is simulated as a significant activator of this gene in both conditions,
206 thereby following the same temporal profiles as the regulated gene.

Table 1: MOSim-defined settings for RNA-seq simulation example. ID: Gene identifier; DE: Whether the gene is differentially expressed (TRUE) or not (FALSE); GrX: Type of gene temporal profile in experimental group X; Tmax.GrX: For transitory profiles, time point where the minimum or maximum is reached in the corresponding group X.

ID	DE	Gr1	Gr2	Tmax.Gr1	Tmax.Gr2
ENSMUSG00000097082	TRUE	Tran.Ind.	Tran.Ind.	1.872	1.311
ENSMUSG00000020205	TRUE	Tran.Ind.	Cont.Ind.	2.114	NA
ENSMUSG00000055493	TRUE	Tran.Ind.	Cont.Rep.	3.062	NA
ENSMUSG00000087802	FALSE	Flat	Flat	NA	NA
ENSMUSG00000017204	TRUE	Tran.Ind.	Cont.Rep.	2.610	NA
ENSMUSG00000017221	TRUE	Tran.Ind.	Cont.Ind.	1.359	NA
ENSMUSG00000052726	TRUE	Tran.Ind.	Tran.Ind.	3.178	1.626

Table 2: MOSim-defined settings for ATAC-seq simulation example. ID: Genomic coordinates of ATAC-seq region (chromosome, and start and end positions for chromatin-accessible regions); Gene: Regulated gene; Effect.GrX: Regulatory effect of the ATAC-seq region on gene expression in experimental group X; GrX : temporal profile of the ATAC-seq region in experimental group X.

ID	Gene	Effect.Gr1	Effect.Gr2	Gr1	Gr2
10_11158324_111588448	ENSMUSG00000097082	activator	activator	Trans.Ind.	Trans.Ind.
10_11158324_111588448	ENSMUSG00000020205	activator	NA	Trans.Ind.	Trans.Ind.
10_11358301_11358431	ENSMUSG00000055493	activator	activator	Trans.Ind.	Cont.Rep.
10_11358301_11358431	ENSMUSG00000087802	NA	NA	Trans.Ind.	Cont.Rep.
11_98682094_98682786	ENSMUSG00000017204	repressor	activator	Trans.Rep.	Cont.Rep.
11_98682094_98682786	ENSMUSG00000017221	repressor	repressor	Trans.Rep.	Cont.Rep.
1_140257767_140257897	ENSMUSG00000052726	activator	activator	Trans.Rep.	Trans.Ind.

208 We applied the K-means method to cluster simulated gene profiles, aiming to verify that the
209 algorithm generates the expected profiles. Features with an average expression per condition
210 of less than one count per million were filtered out. We compared the MOSim assigned profile
211 with the average profile of the corresponding cluster and classified a gene as correctly
212 simulated if both profiles coincided (for example, if a gene was assigned a constant induction
213 profile and clustered with a group exhibiting a continuous increase in expression). The optimal
214 number of clusters was found to be $k = 7$ for K-means clustering, which resulted in one cluster
215 per simulated pattern and time point of maximal or minimal expression. Figure 2A displays the
216 K-means clustering results for the simulated RNA-seq data in group 1, revealing that most
217 genes in the cluster faithfully follow the mean cluster profile, as expected. Overall, less than
218 0.5% of the simulated profiles were assigned to an incorrect cluster.

219 We further evaluated the simulated data using Principal Component Analysis (PCA). The PCA
220 score plot (Figure 2B) indicates that the simulated data effectively recapitulated a quality time
221 course dataset, where replicates were clustered together and consecutive time points were
222 proximate.

223 Following the validation of individual omic data, relationships between gene expression and
224 regulatory omics were evaluated by measuring correlations. An interaction between a regulator
225 and a gene is expected to yield a high absolute correlation value when the regulator exerts a
226 modelled effect on the gene, sharing the same profile type for activation or exhibiting an
227 opposite pattern (i.e., continuous induction vs continuous repression) for repression. When no
228 effect is modelled between the gene and regulator, the profiles will exhibit uncorrelated patterns
229 (e.g. transitory vs continuous). Pearson's correlations were calculated for each interaction and
230 separately for each group. Interactions involving transitory profiles in both the regulator and
231 the gene may include a delayed response, where the signal maxima -or minima- occur at
232 different time points, with Pearson's correlation failing to capture these regulatory

233 relationships. To address these scenarios, we also computed a lagged correlation, limiting the
234 sliding of time points to a maximum of two to control for false positives, and selecting the
235 maximum value from Pearson and lagged correlations as the correct measure. In the ATAC-
236 seq example (Figure 2C), 99.4% of interactions with a modelled activator or repressor effect
237 displayed a correlation value above 0.9, while 0% of interactions without a modelled effect
238 reached this threshold. Correlation values varied widely for these "no effect" interactions,
239 ranging from the expected low values to relatively high ones. The latter can often be attributed
240 to partial overlap between non-comparable profiles, such as a transient induction profile in the
241 gene alongside a continuous induction profile in the regulator, both sharing an increasing linear
242 trend over the same time points. This pattern aligns with the algorithm's intended and expected
243 behaviour. Figure 2D presents simulated temporal profiles for each experimental group,
244 showcasing two randomly selected gene-regulator pairs. In the first pair (top plots), the
245 regulation is activation in both groups, while in the second pair (bottom plots), the regulation
246 is repression, also consistent across both groups.

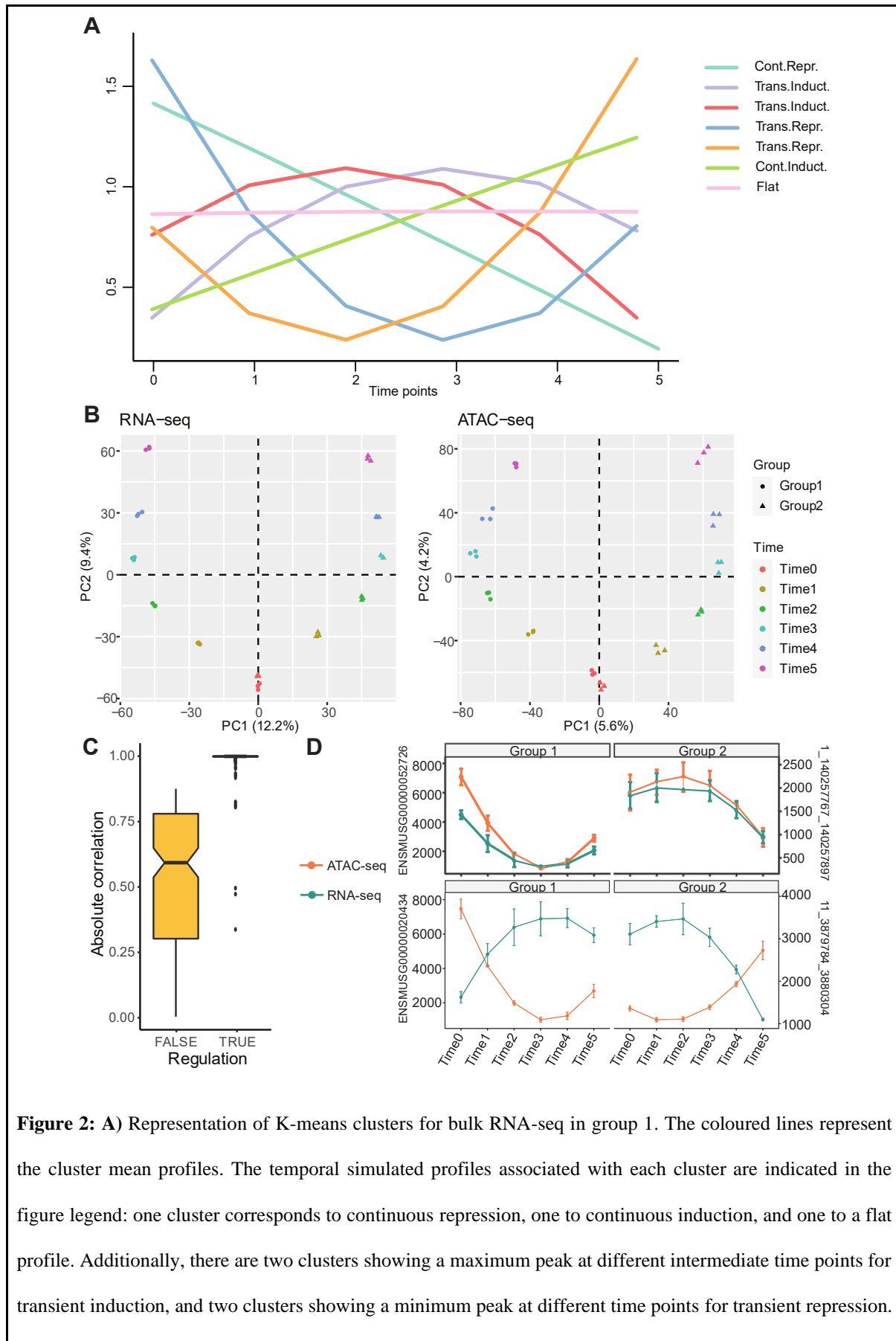


Figure 2: A) Representation of K-means clusters for bulk RNA-seq in group 1. The coloured lines represent the cluster mean profiles. The temporal simulated profiles associated with each cluster are indicated in the figure legend: one cluster corresponds to continuous repression, one to continuous induction, and one to a flat profile. Additionally, there are two clusters showing a maximum peak at different intermediate time points for transient induction, and two clusters showing a minimum peak at different time points for transient repression.

B) Exploratory analysis using Principal Component Analysis on low-count filtered data with logarithmic transformation. The first principal component separates the samples by the experimental group, while the second summarises the temporal profile. X- and Y-axis labels indicate the percentage of variability explained by the corresponding principal component. **C)** Boxplot of absolute Pearson's correlation values from interactions of ATAC-seq regulators with genes in Group 1. Regulation is TRUE when the regulator has been simulated to activate or repress gene expression. Regulation is FALSE for interactions where the regulator has not been simulated to affect gene expression. **D)** Two random examples of gene-regulator temporal profiles in each group. The left Y-axis shows gene expression values, while the right Y-axis shows counts for ATAC-seq regions. Vertical bars at each time point show the standard deviation of the 3 simulated replicates.

247

248 Validation of the single-cell (sc_mosim) simulation approach

249 To demonstrate the utilities of sc_mosim for single-cell sequencing data, we simulated scRNA-
250 seq and scATAC-seq data with six cell types, two experimental groups, and three replicates.
251 We used the pbmcMultiome dataset available from SeuratData [13] as seed data and the gene-
252 regulator association list provided in the MOSim R package. We set the number of DEGs to
253 30% upregulated and 20% downregulated. Variances were set to 0.1 between replicates and
254 0.3 between experimental groups, and we allowed for the modelling of co-expression patterns
255 across cell types, following seven random profiles. Finally, we defined 20% activator and 10%
256 repressor regulators in Group 1, and 10% activators and 20% repressors in Group 2.

257 In single-cell simulations, MOSim generates two main types of output. The sc_omicResults
258 function retrieves a list containing the simulated data matrices for each omic, experimental
259 group and biological replicate, with features in rows and cells in columns. The second results
260 object, extracted with the sc_omicSettings function, includes the MOSim-generated settings
261 that associate genes and peaks (Table 3), and specify TFs with their target genes, along with

262 the type of regulatory relationship between them. For example, gene PTPN22 is identified as
263 an upregulated DEG that follows the across-cell-type expression pattern 5 (Figure 3A). The
264 chromatin-accessible region chr12-31742761-31743451 is modelled as a significant activator
265 of this gene, following the same across-cell-type profile as the regulated gene. Conversely, the
266 association between the gene RBP7 and chromatin-accessible region chr3-101753518-
267 101753798 exemplifies a repressor effect of the regulator omic, where gene and peak follow
268 opposite patterns (clusters 2 and 5, respectively), with the gene downregulated when the
269 regulator is upregulated (Table 3).

Table 3: MOSim-defined settings for scRNA-seq and scATAC-seq for the simulation example. Gene_ID: Gene identifier; Peak_ID: Peak identifier; RegEffect: Regulatory effect of the scATAC-seq region on gene expression in experimental Group 2; G_cluster: gene expression profile across cell types; P_cluster: peak accessibility profile across cell types; G_DE: how the gene is differentially expressed; P_DE: how the peak is differentially accessible. G_FC: Fold Change applied to induce differential gene expression in Group 2 compared to Group 1; P_FC: Fold Change applied to induce differential peak accessibility in Group 2 compared to Group 1.

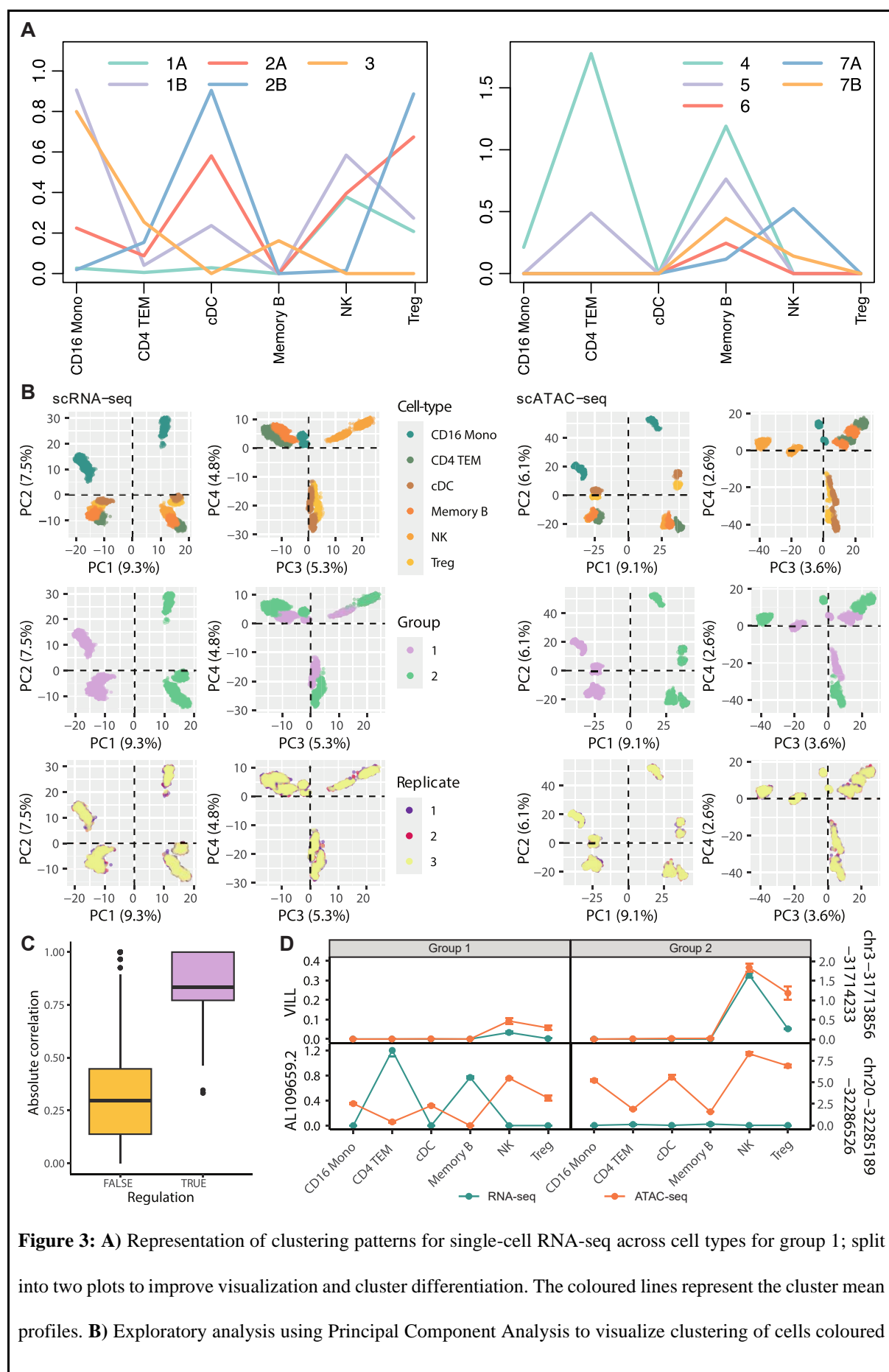
Gene_ID	Peak_ID	RegEffect	G_cluster	P_cluster	G_DE	P_DE	G_FC	P_FC
PRXL2B	chr19-46542333-46543301	Activator	1	1	Up	Up	67.443	67.443
SPSB1	chr22-39902952-39911753	Activator	7	7	Up	Up	73.932	73.932
PTPN22	chr12-31742761-31743451	Activator	5	5	Up	Up	45.054	45.054
PLEKHG5	chr2-132267871-132268833	Repressor	2	5	Down	Up	0.135	57.516
RBP7	chr3-101753518-101753798	Repressor	2	5	Down	Up	0.159	88.201
FRRS1	chr2-88765163-88766080	Repressor	2	5	Down	Up	0.203	74.137

270
271 To demonstrate the robustness of the single-cell MOSim framework for GRN simulation, we
272 assessed its capacity to generate the expected across-cell-type expression profiles. Single-cell
273 data is typically characterised by a high abundance of zeros and many cells belonging to the
274 same cell type, leading to increased noise and outliers. Given the robustness of Spearman's
275 correlation distance and K-medoids clustering techniques in noisy scenarios, we used them to

276 extract and cluster the simulated feature profiles across cell types. The cluster average profiles
277 were then compared to the sc_mosim simulated profiles after excluding genes with flat
278 expression profiles. A feature was deemed correctly simulated if both profiles matched. To
279 achieve this, we set the optimal number of clusters to $K = 10$ for K-medoids clustering, which
280 resulted in one or two clusters per simulated co-expression pattern, minus flat expression.
281 Clustering of the simulated scRNA-seq and scATAC-seq revealed that most features closely
282 adhered to the mean cluster profiles as expected (Figure 3A), with only 3.3% of simulated
283 profiles assigned to an incorrect cluster.

284 We further assessed whether cells from the same cell types, experimental groups, and
285 biological replicates clustered according to the defined simulation settings using PCA for
286 dimensionality reduction (Figure 3B). PCA results showed robust clustering of the simulated
287 data, capturing a high-quality single-cell dataset where PC1 separated cells by experimental
288 group, while PCs 1 to 4 represented the cohesive clustering of cell types (Figure 3B).
289 Additionally, while the majority of data variability was due to differences specified between
290 groups, small variability between biological replicates was also observable (Figure 3B).

291 To evaluate whether simulated regulatory relationships presented stronger correlations than
292 non-regulatory peak-gene associations, Kendall's correlations between gene and peak profiles
293 were computed within each simulated experimental group. A strong absolute correlation is
294 expected for pairs when a regulatory effect was modelled, reflecting similar activation or
295 opposite repression profiles. In contrast, non-regulatory peak-gene interactions typically
296 display lower and more variable correlation values due to differences in absolute terms. As
297 shown in Figure 3C, 79.5% of interactions with modelled activator or repressor effects had
298 absolute correlation values exceeding 0.7, while “no effect” interactions displayed a broader
299 range, centered at 0.32 absolute correlation. This range is likely due to partial overlaps, such
300 as shared trends between cell types, which are expected outcomes of the simulation.



by cell type, experimental group and replicate. X- and Y- axis labels indicate the percentage of variability explained by the corresponding principal component. **C)** Boxplot of absolute Kendall correlation values from interactions of scRNA-seq genes in Group 1 with scATAC-seq regulators. Regulation is TRUE when the regulator has been simulated to activate or repress gene expression. Regulation is FALSE for interactions where the regulator has not been simulated to affect gene expression. **D)** Two examples of gene-regulator single-cell simulated profiles in each group. The left Y-axis shows gene expression values, while the right Y-axis shows counts for scATAC-seq regions. Vertical bars at each time point show the standard error of the mean of the cells for the 3 simulated replicates.

301

302 Finally, Figure 3D illustrates simulated feature profiles across cell types for two pairs of gene-
303 regulator associations, one with an activator effect and the other with a repressor effect. The
304 first regulation (top plots) represents activation in both groups, whereas the second regulation
305 (bottom plots) represents repression across both groups.

306 Simulation of multilayered Gene Regulatory Networks

307 Finally, we illustrate how MOSim effectively simulates multilayered GRNs. Simulating GRNs
308 is challenging due to the complex many-to-many relationships among some regulators and their
309 target genes. For example, a TF or microRNA might regulate multiple target genes with varying
310 regulatory relationships, while the same gene could be influenced by multiple factors. A
311 multimodal GRN simulation algorithm must therefore produce a consistent dataset with
312 expression patterns reflecting these different regulatory patterns. In MOSim, users can specify
313 a desired percentage of active regulatory relationships, and the algorithm adjusts regulatory
314 pairs and profiles to achieve this level of regulation across layers (Figures 2 and 3).

315 To demonstrate MOSim's capabilities in modelling multilayered regulatory interactions, we
316 used the STATEGRA dataset [12] to simulate RNA-seq, miRNA-seq, and TF data. The

317 simulation was performed with a sequencing depth of 30 million reads, two experimental
318 groups, three replicates per group, and six time points, forming a detailed experimental design.
319 Additionally, we specified that 5% of genes be differentially expressed, and 40% of miRNA-
320 seq over the total number of regulators should be repressor effects.

321 Given the complexity of visualising the simulated GRN, we selected the first 100 differentially
322 expressed genes and plotted their corresponding GRNs for each experimental group (Figures
323 4A and 4B). To illustrate the profiles of features in these simulated subnetworks and the
324 efficiency of MOSim in creating consistent expression patterns across different layers, we
325 generated heatmaps for each experimental group (Figure 4C). To facilitate visualisation and
326 interpretation, we calculated the mean expression across replicates for each time point and
327 experimental group, scaling the expression values across modalities, since each omic layer may
328 have different value ranges. Figure 4C demonstrates MOSim's capacity to simulate distinct
329 feature profiles across layers, accurately reflecting both activator and repressor regulatory
330 effects.

331

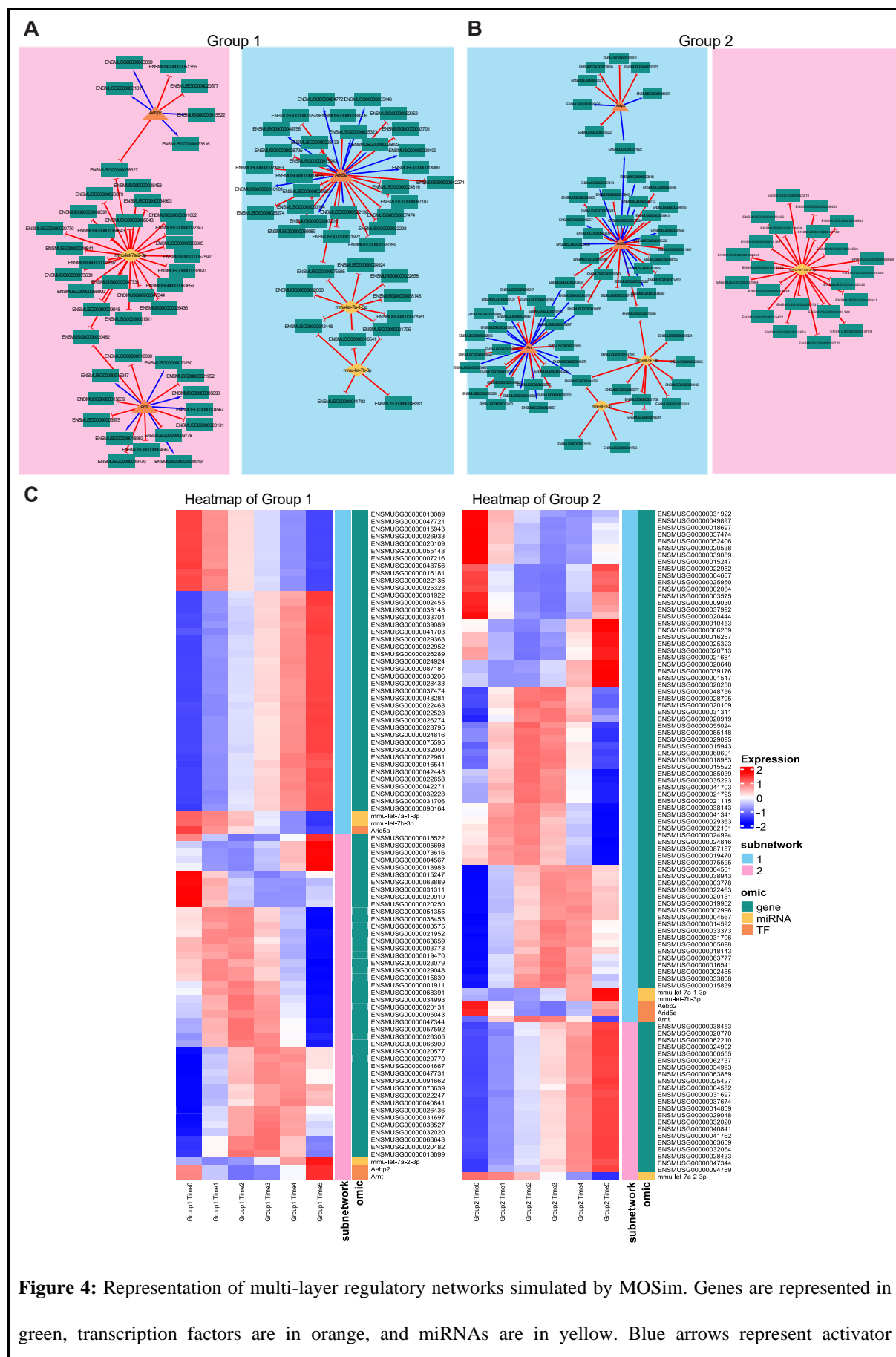


Figure 4: Representation of multi-layer regulatory networks simulated by MOSim. Genes are represented in green, transcription factors are in orange, and miRNAs are in yellow. Blue arrows represent activator

regulations, while red arrows repressor regulations. **A)** Gene Regulatory Network for Group 1. **B)** Gene Regulatory Network for Group 2. **C)** Heatmaps for the expression profiles of the genes, miRNAs and Transcription Factors in Gene Regulatory Networks of Groups 1 and 2. The right Y-axis shows the omic data type and the subnetwork they belong to (which refers to the connected subnetworks observed in A) and B) framed in pink and blue rectangles).

332

333 This example demonstrates that MOSim can generate consistent, complex modules with both
334 positive and negative regulatory relationships, spanning multiple layers and including one-to-
335 many and many-to-many interactions—providing a unique capability to simulate the
336 complexity of gene regulation.

337 Application of MOSim for benchmarking a GRN inference tool

338 To demonstrate one potential application of MOSim simulations, we used MOSim-generated
339 data to test MORE (Multi-Omics Regulation), a tool designed to infer GRNs from bulk multi-
340 omics data [14]. Specifically, we simulated RNA-seq, miRNA-seq and TF data with MOSim
341 using the STATegra dataset [12]. The simulation was configured with a sequencing depth of
342 30 million reads, two experimental groups, 20 time points per group, and one replicate per time
343 point. Additionally, we set the percentage of differentially expressed genes to 50%, and the
344 percentage of significant regulations to 60%.

345 Prior to applying MORE, the RNA-seq count matrix was pre-processed. Low-count genes were
346 filtered out with the NOISeq R package [15], using a threshold of 1 count per million. Count
347 data was normalized with the weighted trimmed mean of M-values (TMM) normalisation in
348 the NOISeq package and voom-transformed [16]. Differential expression analysis between
349 groups 1 and 2 was performed with the limma R package [17], yielding 10593 DEGs (FDR <
350 0.05). These DEGs were set as the target omic features required by MORE. The miRNA-seq

351 and TF data were used as the regulatory omics. For GRN inference, we applied the MORE
352 PLS1 option with auto-scaling and Jack-Knife resampling for the selection of significant
353 regulators.

354 MORE fitted 5573 models, one for each gene with potential regulators. The MOSim simulation
355 provided a total of 370,566 potential regulatory interactions (gene-regulator pairs), 47% of
356 which were simulated as significant in at least one of the groups (174,051 in group 1 and
357 174,067 in group 2). These significant regulations served as the ground truth, or positive
358 instances, to evaluate MORE's performance. At a significance level of 0.05, MORE identified
359 233,598 significant regulations in group 1 and 240,474 in group 2 that were compared to the
360 positive instances. The analysis yielded similar error metrics for both groups, with a slightly
361 better performance observed in miRNA-seq compared to TFs. Overall, MORE achieved a
362 sensitivity of 85.5% and an F1-score of 62.9%. These results demonstrate MORE's ability to
363 detect significant regulatory interactions, while also indicating areas where the tool could be
364 improved or where hyperparameter tuning might enhance its performance.

365 This example highlights how MOSim can serve as a reliable ground truth framework for
366 evaluating the performance of GRN inference tools during their development.

367 **Benchmarking scMOSim's scRNA-Seq simulations using a deep 368 learning algorithm**

369 To further demonstrate other applications of MOSim simulations, we tested it using a
370 Variational Autoencoder (VAE)-based tool. VAEs are capable of learning meaningful latent
371 representations of single-cell data. Unlike standard autoencoders, VAEs impose a probabilistic
372 structure on the latent space, enabling more robust feature extraction and better generalization
373 across datasets. This makes VAEs particularly useful for clustering, dimensionality reduction,

374 and transcription factor perturbation analysis[18]. Examples of VAE models for single-cell
375 data include scGen[19], VEGA[20], siVAE[21], scVAE[22], scDHA[23], scVI[24],
376 manatee[25] and ScInfoVAE[26].

377 We tested scMOSim-generated single-cell RNA-Seq data using the VAE-based tool, single-
378 cell Decomposition using Hierarchical Autoencoder (scDHA)[23]. scDHA first removes noise
379 using a non-negative kernel autoencoder and then projects the data into a low-dimensional
380 space using a stacked Bayesian autoencoder. Finally, it applies iterative perturbations to reduce
381 overfitting and create a more generalized representation.

382 We used one replicate from a single experimental group of scRNA-Seq data simulated with
383 scMOSim to evaluate cell clustering with scDHA. The clustering identified five of six
384 simulated cell types, with one cluster combining cDC and Treg cells (Table 4). The Adjusted
385 Rand Index (ARI) score was 0.949, showing high agreement between predicted and true labels.

Table 4: Number of cells per cell-cluster identified using scDHA, compared with ground truth cell type groups simulated using scMOSim.

		scDHA predicted clusters				
		1	2	3	4	5
scMOSim simulated cell types	CD16 Mono	514	0	0	0	0
	CD4 TEM	0	0	0	298	0
	cDC	0	0	198	0	0
	Memory B	0	0	0	1	370
	NK	0	468	0	0	0
	Treg	0	0	162	0	0

386 These results demonstrate scMOSim's, and its underlying algorithm SPARSim's[11], ability
387 to reliably simulate single-cell RNA-Seq ground truth datasets with different cell-types
388 sufficiently distinguishable as to be identified by a VAE algorithm such as scDHA.

389 Discussion

390 Multi-omic assays, facilitated by massively parallel sequencing technologies, have greatly
391 enhanced our ability to profile regulatory mechanisms in biological systems [1,2], leading to
392 a deeper understanding of diseases and model organisms. However, benchmarking studies of
393 bioinformatic tools designed to elucidate multi-layered GRNs by integrating multi-omics
394 datasets have exposed notable discrepancies in library preparation strategies and analysis
395 methods [27]. These discrepancies underscore the complex challenge of accurately identifying
396 GRNs. As multi-omic sequencing continues to gain traction in the study of regulatory
397 mechanisms, there is a pressing need for tools that support rigorous GRN inference assessment.

398 MOSim was developed to provide a robust framework for simulating bulk and single-cell
399 multi-omics data in a controlled setting. Using a seed dataset and a regulator-gene association
400 matrix, MOSim generates realistic simulated count matrices for both bulk and single-cell
401 transcriptomics data, as well as for associated regulatory omics. For bulk data, the simulation
402 is based on the negative binomial distribution, while for single-cell data, it leverages the well-
403 established simulator SPARSim[11]. By using a seed dataset as a reference to infer
404 distributions, MOSim generates count matrices that closely mirror real omic data, offering a
405 more authentic representation than simulators that artificially construct count matrices without
406 a real-data foundation [28].

407 Additionally, MOSim operates at the count matrix level rather than simulating read data,
408 providing a unified framework for generating multi-omics data across different library

409 preparation methods (e.g., SmartSeq2, 10x Genomics). This allows users to select a preferred
410 method as the seed dataset for MOSim, adding flexibility to the simulation process.

411 MOSim enables a fast and effortless generation of bulk and single-cell count data matrices for
412 multiple omic types, supporting flexible experimental designs. Importantly, the algorithm can
413 simulate complex regulatory relationships between gene expression and other molecular
414 components, guided by prior knowledge, such as target mRNA-microRNA associations. This
415 flexibility in defining experimental designs, DEGs, and active regulators makes MOSim a
416 versatile tool for a variety of different applications, including: i) validating methods aimed at
417 modelling complex, multi-layered regulatory networks, ii) benchmarking multi-omics data
418 integration pipelines, iii) benchmarking GRN inference tools [2], iv) evaluating differential
419 expression and accessibility analysis tools [24], v) testing single-cell data clustering methods
420 (Supplementary File 1) [24], vi) evaluating multi-omics visualization tools, vii) testing methods
421 for time-series analysis in RNA-seq data [29], among others. Several tools have already been
422 tested using MOSim simulations, including DEGRE [30], scAI [31], JISAE [32], GR-NIC [33]
423 and scLRTD [34], highlighting MOSim's ability to specify an association matrix for linking
424 regulators with transcripts further allows users to tailor MOSim outputs to align with the
425 intended integration goals of their analysis tools.

426 The MOSim framework has some limitations. Currently, single-cell simulation is restricted to
427 scRNA-seq and scATAC-seq, as these are presently the only two commercially available
428 sequencing techniques that can be simultaneously performed on the same cell. As additional
429 single-cell omics techniques become widely available, extending MOSim to other data types
430 will be straightforward based on its bulk framework. At this point, MOSim is not prepared to
431 simulate GRN with spatial resolution, which could be inferred from spatial multi-omics data.
432 While these datasets are not yet widespread, they might be in the near future. We envision that
433 the flexible MOSim simulation framework could incorporate the spatial information either as

434 covariates of the regulatory model or by modelling cell-to-cell communication signals as an
435 additional regulatory layer. These possibilities are to be explored in future work. Finally, both
436 bulk and single-cell modules are designed to simulate gene regulatory relationships based on
437 sequencing data, limiting applicability to other omics layers like proteomics and metabolomics,
438 which may influence gene regulation in more complex or uncertain ways. Future work will
439 also explore extending MOSim to simulate interactions between gene expression, the
440 proteome, and the metabolome.

441 Conclusion

442 The integration of multi-omics datasets for GRN identification remains a challenging task. We
443 demonstrate that MOSim serves as an essential resource for benchmarking integration tools,
444 filling a critical gap in the multi-omics sequencing field.

445 Methods

446 The MOSim algorithms are introduced in the results section and extended in Supplementary
447 File 1. The algorithms are implemented in R and mainly use R packages dplyr [35], purrr [35],
448 Stats [36], Iranges [37], Seurat [38], SPARSim [11], and adapted scripts from Acorde [10] and
449 WGBSSuite [9].

450

451 **MOSim algorithms assessment**

452 The performance of the MOSim bulk simulation was tested with mouse multi-omics data from
453 the STATegra project [12], while single-cell simulation performance was evaluated using the
454 human pbmc.multiome 10x Genomics dataset from the SeuratData R package [13].

455 For the bulk data, K-means clustering [39] was applied to the simulated feature profiles to
456 assess the correct simulation of temporal expression patterns. For single-cell data, the simulated
457 count matrix was aggregated to obtain the average count per cell type. Spearman' distance (1 -
458 Spearman's correlation [40]) and partition around medoids (K-medoids [41]) clustering were
459 then used to cluster gene expression profiles across cell-types. In both cases, the optimal
460 number of clusters was obtained by combining the maximisation of Silhouette's coefficient and
461 minimising the intra-cluster variability.
462 In both bulk and single-cell simulations, a log transformation ($\log(x + 1)$)[42] was applied to
463 the data. PCA was used to confirm that clustering aligned with the simulation settings. Finally,
464 to validate gene-regulator relationships, Pearson's correlation was computed for bulk data and
465 Kendall's T_b correlation for single-cell data [43]. These correlations were compared with
466 20.000 random feature pairs with no simulated regulatory effects.

467 Availability of data and materials

468 The package is released under the GNU Public License to the community as a package named
469 MOSim, for Multi-Omics Simulator, at Bioconductor
470 (<https://bioconductor.org/packages/MOSim/>).

471 Bulk example data in MOSim was generated by the STATegra project [12]. Single-cell
472 example data is available in the pbmc.multiome dataset in the SeuratData R package [13]. Code
473 to reproduce the figures in the manuscript is available on github
474 (https://github.com/BiostatOmics/MOSim_plots).

475 Competing interests

476 The authors declare no competing interests.

477 Funding

478 This work was supported by the Scientific Foundation of the Spanish Association Against
479 Cancer through the project PERME224336TARA and by Instituto de Salud Carlos III through
480 the project AC22/00058 (co-funded by the European Union as part of the Next Generation EU
481 programme and the Recovery and Resilience Mechanism, MRR), both projects under the frame
482 of ERA PerMed (ERAPERMED2022-141 - OVA-PDM). This work also received funding
483 from the FP7 STATegra project (agreement no. 306000), the Spanish MINECO (BIO2012-
484 40244), the Spanish MICIN (PID2020-119537RB-100), the Spanish Bioinformatics Institute
485 support (PT17/0009/0015-ISCIII-SGEFI/ERDF), the Scientific Foundation of the Spanish
486 Association Against Cancer (PERME224336TARA), under the frame of ERA PerMed
487 (ERAPERMED2022-141 - OVA-PDM), and the European Union's programme Horizon
488 Europe under a Marie Skłodowska-Curie grant (101149931).

489 Acknowledgements

490 The authors thank Arianna Febbo for preliminary analyses. The development of the tool and
491 test simulations were performed on the high-performance computing cluster Garnatxa at the
492 Institute for Integrative Systems Biology (I2SysBio), I2SysBio is a mixed research centre
493 formed by the University of Valencia (UV) and Spanish National Research Council (CSIC).

494 Author contributions

495 S.T., A.C. and C.M.M. conceptualised and designed the mosim approach. S.T., A.C., C.M. and
496 A.A.L. conceptualised the sc_mosim approach. C.M.M. developed and implemented mosim.
497 C.M. developed and implemented sc_mosim and contributed to implementing mosim. C.M.M.,
498 C.M., M.A. and S.T. performed the analysis and generated visualisations. A.A.L. contributed
499 to implementing sc_mosim. S.T. and A.C. envisioned the study and supervised the work. C.M.,
500 C.M.M., A.C. and S.T. drafted the manuscript. All authors read and approved the final
501 manuscript.

502 Author Biographies

503 Carolina Monzó is a postdoctoral researcher at the Institute for Integrative Systems Biology,
504 Spanish National Research Council (CSIC-UV). Her research interests include
505 bioinformatics, transcriptomics and biology of aging.

506 Maider Aguerralde is a PhD student at the Universitat Politècnica de València. Her research
507 interests include method development, bioinformatics, statistics and multi-omics.

508 Carlos Martínez-Mira is a senior bioinformatics software engineer in Biobam Bioinformatics.
509 His research interests include bioinformatics, statistics and software development.

510 Ángeles Arzalluz-Luque was a PhD student at the Institute for Integrative Systems Biology
511 and Universitat Politècnica de València. Currently, she is a postdoctoral fellow at the Institute
512 of Neuroscience, Spanish National Research Council (CSIC-UMH). Her research interests
513 include bioinformatics, single cell and long-reads transcriptomics analysis.

514 Ana Conesa is a research professor at the Institute for Integrative Systems Biology, Spanish
515 National Research Council (CSIC-UV). Her research interests include method development,
516 bioinformatics and transcriptomics.
517 Sonia Tarazona is an associate professor at the Universitat Politècnica de València. Her
518 research interests include method development, bioinformatics, statistics and multi-omics.

519 **References**

- 520 1. Marku M, Pancaldi V. From time-series transcriptomics to gene regulatory networks: A review on
521 inference methods. *PLoS Comput. Biol.* 2023; 19:e1011254
- 522 2. Badia-I-Mompel P, Wessels L, Müller-Dott S, et al. Gene regulatory network inference in the era of
523 single-cell multi-omics. *Nat. Rev. Genet.* 2023; 24:739–754
- 524 3. Chalise P, Raghavan R, Fridley BL. InterSIM: Simulation tool for multiple integrative ‘omic
525 datasets’. *Comput. Methods Programs Biomed.* 2016; 128:69–74
- 526 4. Chung R-H, Kang C-Y. A multi-omics data simulator for complex disease studies and its
527 application to evaluate multi-omics data analysis methods for disease classification. *Gigascience*
528 2019; 8:
- 529 5. Angelin-Bonnet O, Biggs PJ, Baldwin S, et al. sismonr: simulation of in silico multi-omic networks
530 with adjustable ploidy and post-transcriptional regulation in R. *Bioinformatics* 2020; 36:2938–2940
- 531 6. Song D, Wang Q, Yan G, et al. scDesign3 generates realistic in silico data for multimodal single-
532 cell and spatial omics. *Nat. Biotechnol.* 2023;
- 533 7. Li H, Zhang Z, Squires M, et al. scMultiSim: simulation of multi-modality single cell data guided
534 by cell-cell interactions and gene regulatory networks. *bioRxiv* 2022;
- 535 8. Zinati Y, Takiddeen A, Emad A. GRouNdGAN: GRN-guided simulation of single-cell RNA-seq
536 data using causal generative adversarial networks. *Nat Commun* 2024; 15:4055
- 537 9. Rackham OJL, Dellaportas P, Petretto E, et al. WGBSSuite: simulating whole-genome bisulphite
538 sequencing data and benchmarking differential DNA methylation analysis tools. *Bioinformatics* 2015;
539 31:2371–2373
- 540 10. Arzalluz-Luque A, Salguero P, Tarazona S, et al. acorde unravels functionally interpretable
541 networks of isoform co-usage from single cell data. *Nat. Commun.* 2022; 13:1828
- 542 11. Baruzzo G, Patuzzi I, Di Camillo B. SPARSim single cell: a count data simulator for scRNA-seq
543 data. *Bioinformatics* 2020; 36:1468–1475
- 544 12. Gomez-Cabrero D, Tarazona S, Ferreirós-Vidal I, et al. STATegra, a comprehensive multi-omics
545 dataset of B-cell differentiation in mouse. *Sci Data* 2019; 6:256
- 546 13. Satija Lab L. pbmcMultiome.SeuratData: 10X Genomics PBMC Multiome Dataset. 2022;
- 547 14. Aguerralde-Martin M, Clemente-Ciscar M, Lopez-Cárcel L, et al. MORE interpretable multi-omic
548 regulatory networks to characterize phenotypes. *bioRxiv* 2024;
- 549 15. Tarazona S, Furió-Tarí P, Turrà D, et al. Data quality aware analysis of differential expression in
550 RNA-seq with NOISeq R/Bioc package. *Nucleic Acids Res* 2015; 43:e140
- 551 16. Law CW, Chen Y, Shi W, et al. voom: Precision weights unlock linear model analysis tools for
552 RNA-seq read counts. *Genome Biol* 2014; 15:R29
- 553 17. Ritchie ME, Phipson B, Wu D, et al. limma powers differential expression analyses for RNA-
554 sequencing and microarray studies. *Nucleic Acids Res* 2015; 43:e47
- 555 18. Brendel M, Su C, Bai Z, et al. Application of Deep Learning on Single-cell RNA Sequencing Data
556 Analysis: A Review. *Genomics Proteomics Bioinformatics* 2022; 20:814–835
- 557 19. Lotfollahi M, Wolf FA, Theis FJ. scGen predicts single-cell perturbation responses. *Nat Methods*

558 2019; 16:715–721
559 20. Seninge L, Anastopoulos I, Ding H, et al. VEGA is an interpretable generative model for inferring
560 biological network activity in single-cell transcriptomics. *Nat Commun* 2021; 12:5684
561 21. Choi Y, Li R, Quon G. siVAE: interpretable deep generative models for single-cell
562 transcriptomes. *Genome Biol* 2023; 24:29
563 22. Grønbech CH, Vording MF, Timshel PN, et al. scVAE: variational auto-encoders for single-cell
564 gene expression data. *Bioinformatics* 2020; 36:4415–4422
565 23. Tran D, Nguyen H, Tran B, et al. Fast and precise single-cell data analysis using a hierarchical
566 autoencoder. *Nat Commun* 2021; 12:1029
567 24. Svensson V, Gayoso A, Yosef N, et al. Interpretable factor models of single-cell RNA-seq via
568 variational autoencoders. *Bioinformatics* 2020; 36:3418–3421
569 25. Yang Y, Seninge L, Wang Z, et al. The manatee variational autoencoder model for predicting
570 gene expression alterations caused by transcription factor perturbations. *Sci Rep* 2024; 14:11794
571 26. Pan W, Long F, Pan J. ScInfoVAE: interpretable dimensional reduction of single cell transcription
572 data with variational autoencoders and extended mutual information regularization. *BioData Min*
573 2023; 16:17
574 27. Luecken MD, Büttner M, Chaichoompu K, et al. Benchmarking atlas-level data integration in
575 single-cell genomics. *Nat. Methods* 2022; 19:41–50
576 28. Cao Y, Yang P, Yang JYH. A benchmark study of simulation methods for single-cell RNA
577 sequencing data. *Nat. Commun.* 2021; 12:6911
578 29. Äijö T, Butty V, Chen Z, et al. Methods for time series analysis of RNA-seq data with application
579 to human Th17 cell differentiation. *Bioinformatics* 2014; 30:i113–20
580 30. Terra Machado D, Bernardes Brustolini OJ, Côrtes Martins Y, et al. Inference of differentially
581 expressed genes using generalized linear mixed models in a pairwise fashion. *PeerJ* 2023; 11:e15145
582 31. Jin S, Zhang L, Nie Q. scAI: an unsupervised approach for the integrative analysis of parallel
583 single-cell transcriptomic and epigenomic profiles. *Genome Biol* 2020; 21:25
584 32. Wang C, O’Connell MJ. Autoencoders with shared and specific embeddings for multi-omics data
585 integration. *bioRxiv* 2024;
586 33. Zhang S, Kong W. An improved multiomics data clustering algorithm based on graph
587 regularization constraints. *Third International Conference on Biomedical and Intelligent Systems (IC-
588 BIS 2024)* 2024;
589 34. Ni Z, Zheng X, Zheng X, et al. scLRTD : A Novel Low Rank Tensor Decomposition Method for
590 Imputing Missing Values in Single-Cell Multi-Omics Sequencing Data. *IEEE/ACM Trans Comput
591 Biol Bioinform* 2022; 19:1144–1153
592 35. Wickham H, Averick M, Bryan J, et al. Welcome to the tidyverse. *J. Open Source Softw.* 2019;
593 4:1686
594 36. . R: A Language and Environment for Statistical Computing : Reference Index. 2010;
595 37. Lawrence M, Huber W, Pagès H, et al. Software for computing and annotating genomic ranges.
596 *PLoS Comput. Biol.* 2013; 9:e1003118
597 38. Hao Y, Hao S, Andersen-Nissen E, et al. Integrated analysis of multimodal single-cell data. *Cell*
598 2021; 184:3573–3587.e29
599 39. Hartigan JA, Wong MA. Algorithm AS 136: A K-means clustering algorithm. *J. R. Stat. Soc. Ser.
600 C Appl. Stat.* 1979; 28:100
601 40. Zar JH. Spearman rank correlation: Overview. *Wiley StatsRef: Statistics Reference Online* 2014;
602 41. Reynolds AP, Richards G, de la Iglesia B, et al. Clustering rules: A comparison of partitioning and
603 hierarchical clustering algorithms. *J. Math. Model. Algorithms* 2006; 5:475–504
604 42. Choudhary S, Satija R. Comparison and evaluation of statistical error models for scRNA-seq.
605 *Genome Biol.* 2022; 23:27
606 43. Kendall MG. The treatment of ties in ranking problems. *Biometrika* 1945; 33:239–251
607